《原子核物理评论》
www.npr.ac.cn Nuclear Physics Review
Started in 1984

测量宇生μ子寿命验证堆积事例处理新方法

廖健 余涛 周逸行 徐宇 陈羽 唐健

An Improved Treatment of Pile-up Events Demonstrated by a Cosmic Muon Lifetime Measurement Experiment

LIAO Jian, YU Tao, ZHOU Yixing, XU Yu, CHEN Yu, TANG Jian

在线阅读 View online: https://doi.org/10.11804/NuclPhysRev.39.2021039

引用格式:
廖健, 余涛, 周逸行, 徐宇, 陈羽, 唐健. 测量宇生μ子寿命验证堆积事例处理新方法[J]. 原子核物理评论, 2022, 39(1):73-80. doi: 10.11804/NuclPhysRev.39.2021039
LIAO Jian, YU Tao, ZHOU Yixing, XU Yu, CHEN Yu, TANG Jian. An Improved Treatment of Pile-up Events Demonstrated by a Cosmic Muon Lifetime Measurement Experiment[J]. Nuclear Physics Review, 2022, 39(1):73-80. doi: 10.11804/NuclPhysRev.39.2021039

您可能感兴趣的其他文章

Articles you may be interested in

π^0介子寿命的实验研究

Experimental Research of Neutral Pion Lifetime

原子核物理评论. 2021, 38(3): 256-264 https://doi.org/10.11804/NuclPhysRev.38.2021028

宇生核素 ^{10}Be、^{7}Be、^{22}Na大气示踪概述

Overview of Atmospheric Tracing by Using Cosmogenic Nuclides of ^{10}Be, ^{7}Be, ^{22}Na

原子核物理评论. 2021, 38(3): 277-282 https://doi.org/10.11804/NuclPhysRev.38.2020073

超氚核寿命之谜及其展望(英文)

Hypertriton Lifetime Puzzle and Its Perspective

原子核物理评论. 2019, 36(3): 273-277 https://doi.org/10.11804/NuclPhysRev.36.03.273

放射性核素寿命计算方法的模拟研究

Simulation Study of Lifetime Calculation Methods for Radioactive Nuclides

原子核物理评论. 2020, 37(3): 611-616 https://doi.org/10.11804/NuclPhysRev.37.2019CNPC26

不稳定原子核β衰变强度的实验测量方法

Experimental Measurement Method of Beta Decay Strength of Unstable Nuclei

原子核物理评论. 2020, 37(3): 438-446 https://doi.org/10.11804/NuclPhysRev.37.2019CNPC69

τ 轻子衰变及其应用

τ Lepton Decays and Applications

原子核物理评论. 2020, 37(3): 698-704 https://doi.org/10.11804/NuclPhysRev.37.2019CNPC24

Article ID: 1007-4627(2022)01–0073–08

An Improved Treatment of Pile-up Events Demonstrated by a Cosmic Muon Lifetime Measurement Experiment

LIAO Jian, YU Tao, ZHOU Yixing, XU Yu, CHEN Yu†, TANG Jian†

(*School of Physics, Sun Yat-sen University, Guangzhou 510275, China*)

Abstract: A statistical correction method is proposed to suppress the pile-up background events in data analysis. This method is verified by a cosmic muon lifetime measurement experiment, achieved by a plastic scintillator detector using the timing coincidence method, where dominant background events originate from pile up muons and electronic noise. To complement the intrinsic shortcoming of relatively rare decay events from registered cosmic muon events in the local laboratory, Monte Carlo simulation is applied to generate large samples in order to cross check the new method. The measurement of the muon lifetime in our setup gives a result of $\tau_{\mu}^{\rm exp} = 2.19 \pm 0.07$ μs at 95% confidence level, while the result before applying the correction is $\tau'_{\mu} = 2.27 \pm 0.07$ μs (95% C.L.). The treatment of pile-up events by a statistical correction equation in this study might be adapted to improve data analysis in the general coincident background dominating experiments.

Key words: cosmic muon; muon lifetime measurement; coincident backgrounds; pile-up events

CLC number: O571.53 **Document code:** A **DOI:** 10.11804/NuclPhysRev.39.2021039

1 Introduction

The pile-up effect is one of the most notorious enemies in the precision measurement of particle physics experiments. In a large-scale collider experiment, the pile-up effect happens when the interaction of interests is recorded together with the one that we are less interested in, from additional energy contributions in jets to the mis-identified final states, at the limited resolution window. Various beam experiments suffer from pile-up backgrounds such as those of other collisions in current and surrounding bunch crossings, cosmic ray muons, beam-gas, beam-halo, cavern background, detector electronic noise and the alike[1−4]. On the other hand, the suppression of pile-up background events has also been one of crucial components in rare event searching experiments such as SNO+[5], CUPID[6]. It is of vital importance to develop sophisticated techniques to identify and suppress pile-up background events in the particle physics experiments.

Different methods have been implemented to cope with the pile-up events. The CMS collaboration has introduced the charge hadron subtraction and PUPPI(PileUp Per Particle Identification) algorithms to identify the pile-up events[7−8]. The Crystal Zero Degree Detector in BESIII has used a Field Programmable Gate Array(FPGA) to run the waveform analysis program to reject the pile up events[8]. The bottom-up algorithms for this purpose has also been developed[9−10]. In the non-collider physics areas, most experiments have installed the active cosmic muon veto to suppress these pile up events, such as the resistant plate chamber veto in Daya Bay reactor neutrino experiment and the plastic scintillator veto in Angra experiment[11−15].

Most of the aforementioned methods tend to deploy the advanced hardware setup to identify and subtract the pile-up events. However, it is impossible to remove them completely. More often than not, it seems still unclear how each component of pile-up backgrounds contributes to the experimental errors in a systematic manner without underlying physics interpretations. Therefore, we propose a new method, based on the statistical principle, to suppress the pile-up backgrounds in the data analysis. In order to justify the method, a cosmic muon lifetime measurement experiment, whose main source of errors comes from pile-up backgrounds, can be conducted.

In history, precision measurement of the muon lifetime based on an accelerator muon source was first conducted in 1961, where Richard A. Lundy got a result of 2.203 μs, with an relative error of 0.2% (98% C.L.)[16−20]. In 1970, R.E. Hall measured the muon lifetime by using a

Received date: 05 May 2021; **Revised date:** 20 Jun. 2021

Foundation item: National Natural Science Foundation of China(12075326); Undergraduate Teaching Improvement Program in Sun Yat-sen University; National Undergraduate Innovation and Entrepreneurship Training Program(20201319)

Biography: LIAO Jian(2000−), Foshan, Guangdong Province, working on high energy physics; E-mail: liaoj35@mail2.sysu.edu.cn

† **Corresponding author:** CHEN Yu, E-mail: chenyu73@mail.sysu.edu.cn; TANG Jian, E-mail: tangjian5@mail.sysu.edu.cn.

multi-layer inorganic scintillator with the help of cosmic muons[21]. This approach has become more mature after several improvements[22–24]. In 2011, Webber *et al.*[25] got a result of 2.196 980 3 μs with the relative error decreased to 1 ppm (68.3% C.L.). Bearing with less precision and following the precious experience[26–29], it is simple and easy to line up multiple plastic scintillators with Photo-Multiplier Tubes(PMTs) or Silicon Photo-Multipliers (SiPMs) to build a coincidence detector to measure the muon lifetime, though. It must be straightforward to apply the statistical method to deal with the pile-up backgrounds in the muon lifetime measurement experiment①. This article presents our efforts in the local laboratory and demonstrate effectiveness of the statistical method applied to pile-up events.

In Sec. 2, we describe how the statistical method is applied to the pile-up backgrounds. In Sec. 3, the working principle in a muon lifetime measurement is introduced, including the experimental setup, the waveform classification algorithm and background subtraction techniques by means of a statistical method. The experimental results are also validated by the house-hold Monte-Carlo simulation in Sec. 4. Finally, we summarize the work and present prospects of this statistical method to improve the analysis in the general coincident background dominating experiments.

2 Strategy to suppress pile-up backgrounds

We take the muon lifetime measurement experiment as a demonstration. Two plastic scintillators were used to build a coincidence detector, in order to distinguish cosmic muon events from ambient radiation events. Only particles with high enough energy are able to go through both layers of the plastic scintillators almost simultaneously. Since the energy of cosmic muons is $O(1)$ GeV, these particles will penetrate the scintillators with no difficulty and leave simultaneous coincident signals. However, the particles from ambient radiation (α, β and γ), which is one of the major detector noise sources, are of lower energy and will hardly be able to trigger both of the scintillators. The schematic diagram of the coincidence detector and the circuit diagram to readout SiPM signals for such a purpose are shown in Fig. 1 and Fig. 2. First, we will focus on the classification of the event types and their corresponding waveforms. Then, the statistical method will be applied to suppress the pile-up background in the experimental data analysis.

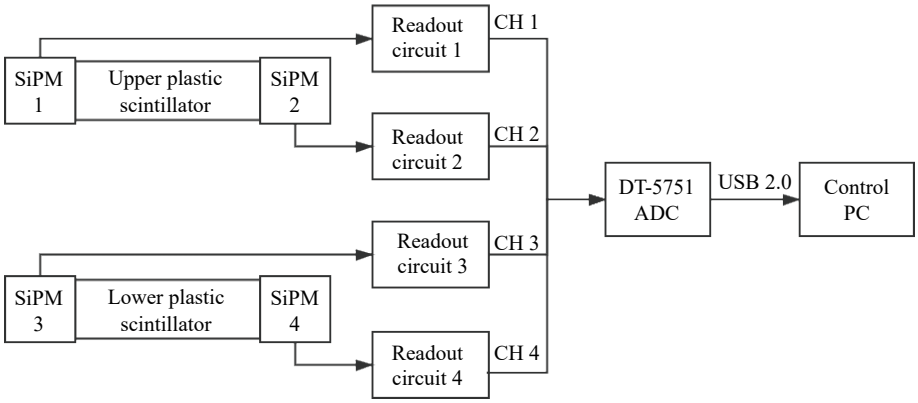

Fig. 1 The schematic diagram of the coincidence detector.

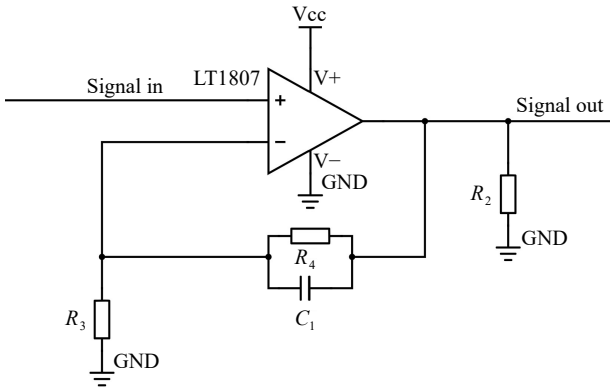

Fig. 2 The schematic diagram of the coincidence detector.

2.1 Classification of pile-up events

To the best of our knowledge, there are mainly two kinds of muon events in the detector scintillators. The first one is the muon coincidence event, which is trivial and less interesting. The second one is the muon decay events. The cosmic muons of proper energy will stop inside the lower scintillator. Muons or antimuons are not stable and can decay into an electron or a positron and neutrino-antineutrino pairs. The decay process of $\mu^{\pm}$ is shown as follows:

$$\mu^{\pm} \rightarrow e^{\pm} + \nu_e(\bar{\nu}_e) + \bar{\nu}_\mu(\nu_\mu). \tag{1}$$

The secondary electron/positron can also ionize in the plastic scintillator and produce a second pulse signal. The

①We have to emphasize here that it is great to check the validity of statistical treatment of pile-up events by means of cosmic muons for the sake of their abundance and availability rather than a competition with the latest high-precision measurement of the muon lifetime based on an accelerator muon source.

time interval Δt between two pulse peaks of the arrival signal caused by a passing muon and the decay signal by Michel electron will shape an exponential distribution ideally as samples for the muon lifetime measurement.

As for the backgrounds, we pay more attention to background sources from cosmic muon pile-up events, electronic noise and ambient radiation induced coincident events. The detector structure indicates that most of high-energy cosmic muons are likely to traverse the lower scintillator panel only. If the time interval between a coincidence event and a single-bottom-hit event is located outside the specified time window T but fall within the sampling range in the readout system, these events are also saved and included in data analysis. However, we have to carefully deal with these pile up events to avoid contamination in the real cosmic muon decay signals. Another noise sources are α, β and γ particles from the ambient radiation. The indoor ambient radioactivity level is set to 100 $\mathrm{Bq/m^3}$, higher than the average levels in China ($\sim$40 $\mathrm{Bq/m^3}$)[30–31]. Taking them into simulation, we immediately realize that these events are extremely rare in the current study and can be safely ignored. The responding mode of the coincidence events, the muon decay events, the muon pile-up events in shown in Fig. 3.

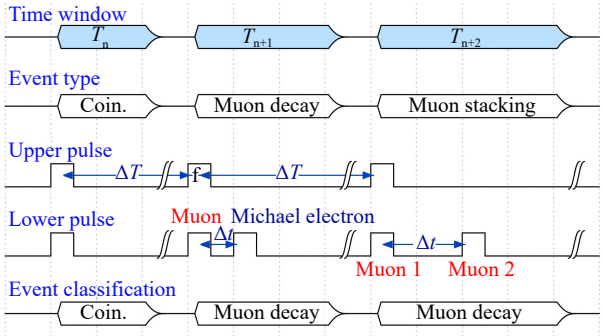

Fig. 3　(color online)The classification of the detector responses. The "Event Type" represents the actual type of an event. The normal muon coincidence events (Coin.), the muon decay events and the muon pile up events are all taken into account. The "Upper pulse" and "Lower pulse" represent the pulse signals generated by the upper and lower scintillator, respectively. An OR logic gate is applied to two channels of each scintillator, in order to maximize the detection efficiency. The "Event Classification" represents the reconstruction of the event type based on the waveform. The record time window is activated once the upper and lower SiPMs are almost simultaneously triggered and will keep recording for 20 μs. If there are 2 pulses within a single time window, the event will be classified as a muon-decay event.

2.2　Statistical method

For simplicity, we can start with a rough estimate on pile-up events in the cosmic muon lifetime measurement experiment. Assuming that the muon events are uniformly distributed in time, the peak distance of pile-up events, denoted as D_{pileup}, will also almost uniformly distributes within the time window, T. Thus, we can estimate that the mean value of D_{pileup} satisfies $\bar{D}_{\mathrm{pileup}} \approx \frac{1}{2}T > \tau_{\mu}$. It means that misidentified pile-up events will lead to a larger value in the muon lifetime result.

In fact, since the muon pile-up events can be treated as two adjacent muon coincidence events with small enough time interval, denoted as ΔT. According to the previous assumption that the detector responses are uniformly distributed in time, ΔT obeys the exponential distribution and the probability distribution function (PDF) is as follows:

$$f_c^{\infty}(t) = \begin{cases} \dfrac{1}{\tau_c}\mathrm{e}^{-t/\tau_c} & (t \in [0,\infty)) \\ 0 & (\text{elsewhere}), \end{cases} \tag{2}$$

where τ_c is arithmetic average of the ΔT samples and determined by data driven analysis.

$$f_c(t) = \begin{cases} \dfrac{1}{A\tau_c}\mathrm{e}^{-t/\tau_c} & (t \in [0,T]) \\ 0 & (\text{elsewhere}), \end{cases} \tag{3}$$

where $A = \int_0^T f_c^{\infty}(t)\mathrm{d}t = 1 - \mathrm{e}^{-T/\tau_c}$, is the normalization factor. The muon lifetime by its definition obeys the exponential distribution. The two PDFs are shown in Fig. 4. According to our assumption, the pile-up events are almost uniformly distributed in the time window T, which means τ_c, the mean value of ΔT satisfies $\tau_c \gg T > \tau_{\mu}$. As a result, the ΔT's PDF is a slow-changing function in $[0,T]$ and acts like a uniform distribution, as shown in the Fig. 4.

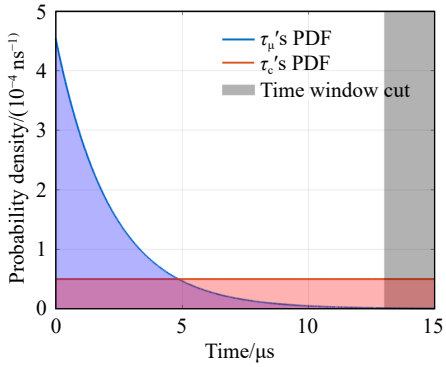

Fig. 4　(color online)Peak Distance's distributions of muon decay events and event pile up effects. The blue line and the red line represent the muon's lifetime distribution and the background events distribution in a given time window $T = 13$ μs, respectively. The gray area is the time window cut.

Let random variables D, c and m represent the peak distance of double-pulse events, pile-up events, muon decay events, respectively. Without a loss of generality, we assume that the muon pile-up and decay events are independent. Allow λ to represent the proportion of muon decay events in all double-pulse events with $\lambda \in (0,1)$. As a

result, the peak distance of double-pulse events D can be expressed in the form of weighted sum of the peak distance of pile-up events and that of muon decay events, whose weight is $1-\lambda$ and λ, respectively, as shown in Eq. (4).

$$D = \lambda m + (1-\lambda)c \equiv M + C, \tag{4}$$

where $M \equiv \lambda m, C \equiv (1-\lambda)c$. Since the PDFs of m and c are clear, one can immediately write down the PDFs of M, C and D, as shown in Eqs. (5)~(7), respectively.

$$f_M(x) = \begin{cases} \dfrac{1}{\tau_1}\mathrm{e}^{-x/\tau_1} & (x \in [0,\infty)) \\ 0 & (\text{elsewhere}), \end{cases} \tag{5}$$

$$f_C(y) = \begin{cases} \dfrac{1}{A\tau_2}\mathrm{e}^{-y/\tau_2} & (y \in [0,T]) \\ 0 & (\text{elsewhere}), \end{cases} \tag{6}$$

$$\begin{aligned} f_D(z) &= \int_{-\infty}^{\infty} f_M(x) f_D(z-x)\mathrm{d}x \\ &= \begin{cases} \dfrac{1}{A(\tau_1-\tau_2)}\left(\mathrm{e}^{-\frac{z}{\tau_1}} - \mathrm{e}^{-\frac{z}{\tau_2}}\right) & (t \in [0,(1-\lambda)T)), \\ \dfrac{1}{A(\tau_1-\tau_2)}\mathrm{e}^{-z/\tau_1}\left\{1-\exp\left[-\dfrac{\tau_1-\tau_2}{\tau_1\tau_2}(1-\lambda)T\right]\right\} & \\ (t \in [(1-\lambda)T,\infty)), & \\ 0 \ \ (\text{elsewhere}). & \end{cases} \end{aligned} \tag{7}$$

The mean value of D is shown in the Eq. (8).

$$\bar{D} \approx E(D) = \int_0^{\infty} z f_D(z)\mathrm{d}z = \tau_1 + \tau_2 - \frac{T(1-\lambda)}{A}\mathrm{e}^{-T/\tau_c}, \tag{8}$$

where $\tau_1 = \lambda\tau_\mu$, $\tau_2 = (1-\lambda)\tau_c$. Finally, we can replace the parameters A and λ with the observable quantities. If we allow N, N_D, N_C and N_μ to represent the number of coincidence events, double-pulse events, noise events, muon decay events, respectively, we will obtain the following equations:

$$N_\mathrm{C} = N\int_0^T f_c^{\infty}(t)\mathrm{d}t = NA, \tag{9}$$

$$N_\mu = \lambda N_\mathrm{D}, \tag{10}$$

$$N_\mathrm{C} = (1-\lambda)N_\mathrm{D}. \tag{11}$$

Using Eqs. (9)~(11) to replace the parameters A and λ, we finally get to the result for τ_μ:

$$\tau_\mu = \frac{\bar{D} + \dfrac{N}{N_\mathrm{D}}T\mathrm{e}^{-T/\tau_c} - \dfrac{N}{N_\mathrm{D}}(1-\mathrm{e}^{-T/\tau_c})\tau_c}{1-\dfrac{N}{N_\mathrm{D}}(1-\mathrm{e}^{-T/\tau_c})}. \tag{12}$$

Keep in mind that $\tau_c \gg T$, $\frac{T}{\tau_c} \ll 1$. In order to interpret the physics in the above formulae, we can expand the term e^{-T/τ_c} in Taylor series. With the numerator to the first order and the denominator to the zeroth order, then one could reach:

$$\tau_\mu \approx \bar{D} - \frac{N}{N_\mathrm{D}}\frac{T^2}{\tau_c}. \tag{13}$$

Eqs. (13) is simplified and relatively elegant. This approximation explicitly shows the outcome of background events represented by the term $\frac{N}{N_\mathrm{D}}\frac{T^2}{\tau_c}$. This term also verifies our initial guess that the effect of pile-up events will lead to a larger value in the lifetime measurement result. It is then easy to understand how to suppress the pile up coincident backgrounds.

3 Cosmic muon lifetime measurement

3.1 Experimental setup

A 2-layer coincidence detector is built to measure the cosmic muon lifetime, as shown in Fig. 5.

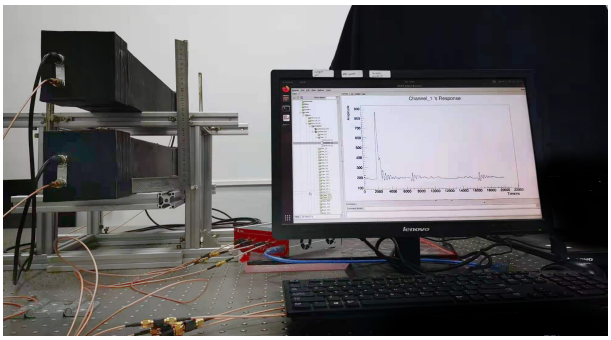

Fig. 5 (color online)Picture of the detector in the local laboratory.

The detector consists of two $60\,\mathrm{cm}\times 60\,\mathrm{cm}\times 10\,\mathrm{cm}$ plastic scintillator panels. Four $6\,\mathrm{mm}\times 6\,\mathrm{mm}$ SiPMs are used to readout scintillation signals. Each SiPM is attached to the end of the scintillator panel with the surface area of $10\,\mathrm{cm}\times 10\,\mathrm{cm}$. To increase the light coupling efficiency, the optical cement is applied between the interfaces. The data acquisition module is CAEN DT-5751, which has 10 bits resolution and 1 GS/s sampling rate.

3.2 Waveform classification algorithm

It is essential for us to record waveforms in a certain time window so that we can determine the signals coming from cosmic muons rather than conincident backgrouds from ambient β or γ partices. In addition, we have to select the potential decay muon events or the so-called "double-bang" events by judging whether there is the second pulse in a waveform in the time region of interests. The trigger level is set to 400 ADC. A coincidence signal is recorded when its amplitude is higher than the trigger level. A dedicated ROOT script is used to loop over all the waveforms to locate the potential muon decay events with two peaks. We have collected thousands of triggered coincident cosmic muons in our system tagged as potential decay

muon samples. The registered double-pulse waveforms can be categorized into three sets: The first one has a single main peak and a ringing peak; the second one contains two separate main peaks; the third one maintains a structure of two main peaks falling in a short time window. The typical waveforms in each set are shown in Fig. 6.

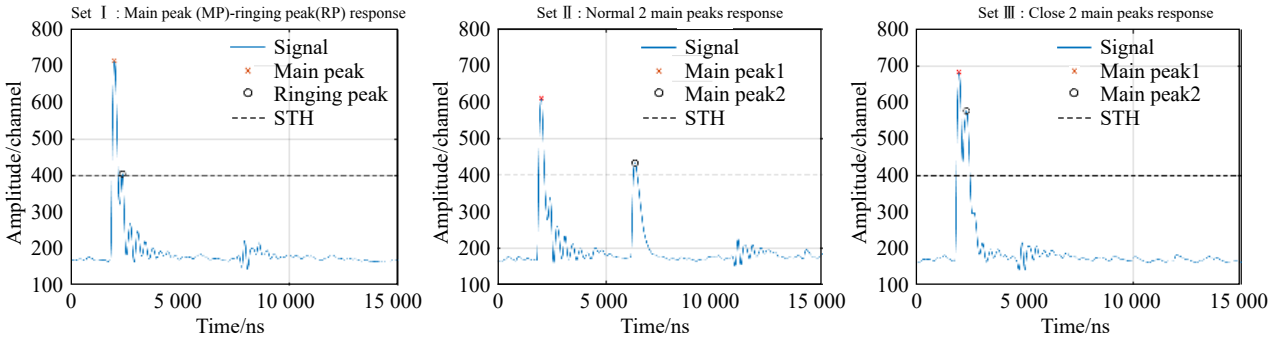

Fig. 6　(color online)The collected double-pulse waveforms from either end of the lower scintillator can be categorized into three sets. Set I waveforms only have a single main peak(MP) and a ringing peak(RP) (MP-RP waveforms), while both Set II and III have 2 main peaks (MP-MP waveforms). The STH represents the static threshold. A double-pulse wavefrom is recorded only if it has at least one peak that higher than STH, the static threshold.

It seems very likely that the single-peak response in Set I was triggered by cosmic muons while the second ringing pulse comes from an electronic noise. Nevertheless, Set II and III are the double-peak response, which we are most interested in. Set I shows that at the falling edge of the main peak, there is a damping oscillation tail called "ringing". The ringing part in the waveform also has a local maximum, which will definitely affect the waveform classification algorithm. It is quite straightforward to look for pulse peaks with the help of a simple static threshold (STH). However, we suffer from ringing and event pile up effect limited by data acquisition system. Especially, a simple static threshold value cannot distinguish Set I and III. To overcome the barrier, we introduce the alternative solution such as a dynamic threshold value (DTH). The STH is only used to distinguish the signal and noise, and the DTH is good at separating samples in Set I, II and III. To get the DTH, we project the first and second pulse amplitudes in the same plane and find that the height of RPs is almost linearly dependent on the corresponding MPs. Therefore, a linear fit is applied to all the MP-RP waveforms, as shown in Fig. 7.

Then, the DTH could be calculated by MP's height and the fit result. Fig. 8 is the schematic diagram of the waveform classification.

3.3　Experimental results

According to the analysis in Sec. 2, τ_c, which is the mean value of the time interval of adjacent responses, is required. Thus, more than 10^6 coincidence events were collected and their time intervals ΔT are filled into a 600-bin histogram. The result is $\tau_c = 0.2265 \pm 0.0003$ s at 95% C.L. The result only includes statistical error. The fit result of ΔT is shown in Fig. 9. Thus, in a finite time window T, the PDF of ΔT is given in Eq. (3).

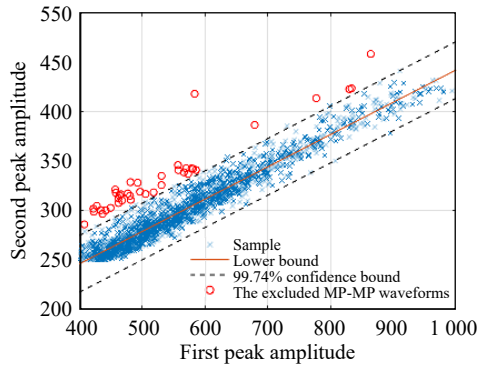

Fig. 7　(color online)The pulse height spectra of the first and the second peaks in the waveforms. The abscissa represent the first peaks'(mostly MP) height and the vertical one represents the second peak's (mostly RP) height. The width of the confidence bound is determined by the range at 3σ C.L. The upper bound is used for the dynamic threshold, DTH. The excluded MP-MP events are represented by red circles.

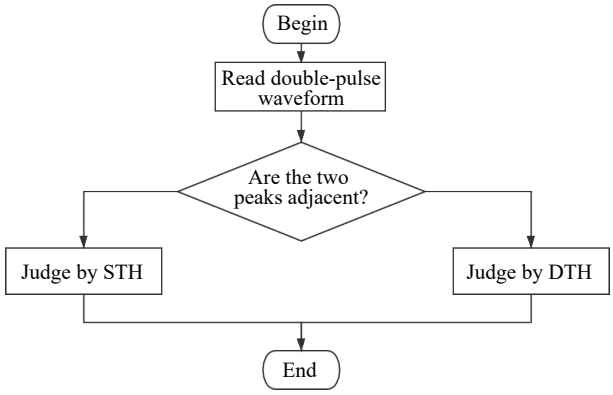

Fig. 8　The flow chart to categorize Set I and III waveforms in Fig. 6. Set I waveforms have adjacent main peaks and ringing peaks, while Set III waveforms have two adjacent main peaks. Hence, Set I waveforms are also recorded and analyzed, though they are not decay signals. To distinguish Set I and III waveforms, the dynamic threshold DTH is introduced.

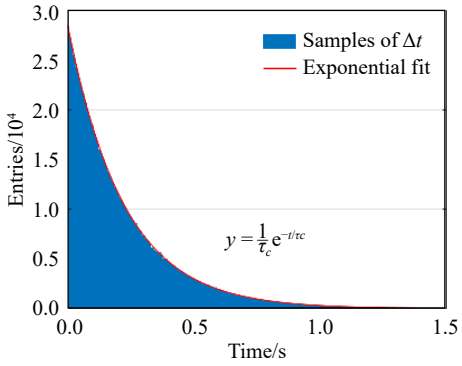

Fig. 9 (color online)The histogram of the time interval ΔT between two detector responses. The red line is the exponential fit. The parameter τ_c is arithmetic average of the ΔT samples, thus it will not be affected by the binning strategy.

The data collection lasted in a month, and approximately 4 918 decay events are recorded. In some samples, only one of the two waveforms from the lower scintillator passed the trigger threshold and were recorded so that the unique peak distance is treated as a muon lifetime sample. In other cases, two waveforms were both recorded and analyzed, resulting in 2 peak distances with the difference at $O(1)$ ns. Therefore, the mean value of two peak distances are treated as a sample to avoid any bias. The time window T is chosen as 13 ms and limited by data acquisition system. The muon lifetime result before the correction is $\tau'_\mu = 2.27 \pm 0.07$ μs. After applying Eq. (12) to the result, we finally obtain: $\tau_\mu^{\rm exp} = 2.19 \pm 0.07$ μs. Only the statistical errors are included here. The uncertainty of $\tau_\mu^{\rm exp}$ comes from the peak distance of double-pulse events D and the arithmetic average of the coincidence time interval in samples τ_c. The discrepancy between $\tau_\mu^{\rm exp}$ and τ'_μ, which is the result of the correction method, is larger than the uncertainty, which represents the statistical fluctuation. On the other hand, the final result $\tau_\mu^{\rm exp}$ is also consistent with the reference value in particle data group (PDG)[32]. It has verified the validity of the correction method in the scenario with potential coincident pile-up backgrounds. The lifetime histogram is shown in Fig. 10.

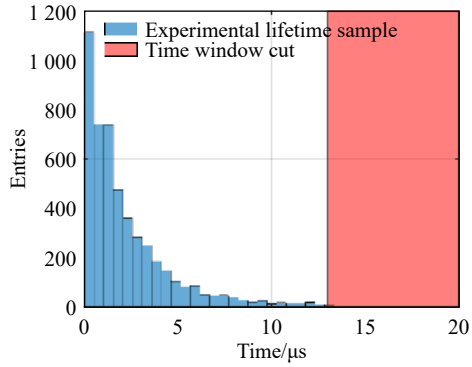

Fig. 10 (color online)The histogram of measured cosmic muon decay samples in the experiment.

4 Monte-Carlo simulation based on GEANT4

4.1 Simulation setup

As it is relatively rare to identify the decay muon events by coincident measurement of cosmic muons, it must be good to check the validity of this statistic correction method by means of large samples by Monte Carlo simulation. For this purpose, we make use of GEANT4 with modularized, ready-to-use physics lists with the class G4ModularPhysicsList[33−35]. The built-in class G4EmStandardPhysics and G4OpticalPhysics are used for Electromagnetic processes and optical processes, respectively. The class G4StoppingPhysics is also used to simulate the μ^- capture, which is verified to be affecting the lifetime of μ^-[36−37]. As for the background study, the pile up events and the ambient radiation events are both simulated. The ambient radiation events are extremely rare, probably due to the high threshold value and the low background radiation intensity in our experimental setup.

4.2 Event generator

The data used for generating cosmic muon spectrum is taken from CAPRICE 94 and CAPRICE 97 experiments[38], whose results have relatively small errors and are in good agreement with other experiments and spectrum shape equations[39−40]. The zenith angle distribution of cosmic muon is described by the shape of $\cos^\alpha\theta$ with $\alpha \approx 2$, which has been verified by multiple measurements[41−42].

4.3 Waveform modeling in SiPM

Geant4 can only track the semi-classic particles that have a well-defined position and momentum. In the simulation program, the generated light signal is a collection of single photoelectrons (SPEs). To reconstruct the actual electronic signal, a conversion algorithm is needed. We have built a model to simulate the waveform of SiPM, based on the single photoelectron response. First of all, a model converting the infinitesimal-width light signal is proposed based on the assumption that SiPM's response is the linear superposition of the SPEs. Second, we apply the model to convert the finite width light signal in the most general case.

The signal of SPE is fitted by a model with a convolution of logarithmic and exponential terms, as is shown in Eq. (14). For simplicity, we can first neglect the width of the light signal. Hence, it becomes the Dirac delta function, $N\delta(t)$, where the parameter N represents the relative light intensity. Since the PN nodes inside a SiPM are in parallel with each other, it is reasonable to assume that if the PN nodes are ignited simultaneously, the total current is the linear superposition of each PN node's current. Therefore, the electronic signal can be writen down by a simple multiplic-

ation, as is shown in Eq. (15).

$$SPE(t) = \frac{A}{t\sigma\sqrt{2\pi}} \exp\left[-\frac{\ln^2\left(\frac{t}{\tau}\right)}{2\sigma^2}\right] + B, \tag{14}$$

$$y(t) = N \times SPE(t), \tag{15}$$

where τ and σ accounts for the central value and the width in the SPE waveform, respectively. A and B represents the amplitude and the baseline of each waveform, respectively. If the light signal has a finite width, which means that photons hit the SiPM at the different time, each hit can be treated as an individual infinitesimal-width light signal and trigger a SPE response. Hence, the reconstructed electronic signal is the linear superposition of all SPE responses. To reduce the computational resources, one can fill the time stamps of photon hits $\{t_i'\}_{i=1}^{N}$ into a histogram and get the bin edges $\{t_i\}_{i=1}^{n}$ and the corresponding bin counts $\{n_i\}_{i=1}^{n}$. Each bin can be treated as a infinitesimal-width light signal $n_i\delta(t-t_i)$. As a result, the light signal $I(t)$ is the superposition of all bins and the reconstructed electronic signal $Y(t)$ is the convolution of SPE waveform $SPE(t)$ and the light signal $I(t)$, as shown in Eq. (16). Fig. 11 shows the typical reconstructed electronic signal.

$$I(t) = \sum_{i=1}^{n} n_i\delta(t-t_i),$$
$$Y(t) = \int_{-\infty}^{\infty} y(t)I(t)\mathrm{d}t = \sum_{i=1}^{n} n_i SPE(t-t_i). \tag{16}$$

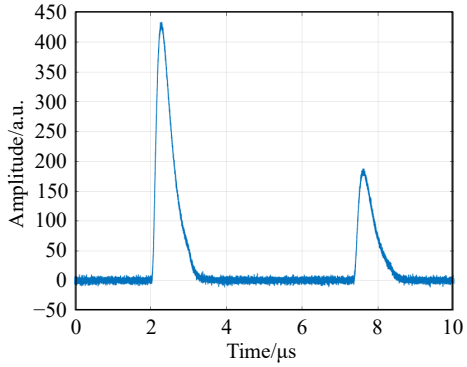

Fig. 11　(color online)The simulated response of muon decay events. The reconstructed electronic signal is convoluted with the electronic noise.

4.4　Simulation result

In total, 33355 double-pulse events in simulation are collected and analyzed. The event pile up effect and the ambient radiation events are also included. After we apply the improved analysis method in the simulated data samples, the result with correction is 2.20 ± 0.03 μs at 95% C.L. while the simulation result without correction gives 2.29 ± 0.03 μs. The results only include the statistical error. The histogram of muon decay spectrum in simulation is shown in Fig. 12. Therefore, the consistency of our result with regards to the reference value in simulation has verified the validity of the correction.

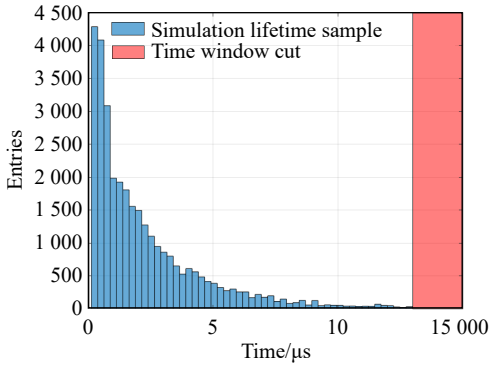

Fig. 12　(color online)The histogram of muon-decay spectrum in simulation.

5　Conclusion

In this study, we have proposed a statistical strategy to cope with pile-up background events in experiments. As a demonstration, we have built a two-layer plastic scintillator detector to collect cosmic muon events and implemented the new correction method to suppress coincident and pile-up backgrounds in the muon lifetime measurement. After data analysis with an improved treatment of pile-up events, we have obtained the muon lifetime as $\tau_{\mu}^{\mathrm{exp}} = 2.19 \pm 0.07$ μs at 95% C.L. The result is consistent with the PDG value and supported by a MC simulation with much larger samples. In the end, we wish that the correction method for pile-up events can help with the general or the similar coincident background dominating experiments.

References:

[1] BERTOLINI D, HARRIS P, LOW M, et al. JHEP, 2014, 10: 059.
[2] AABOUD M, AAD G, ABBOTT B, et al. Eur Phys J C, 2017, 77(9): 580.
[3] ARJONA MARTÍNEZ J, CERRI O, PIERINI M, et al. Eur Phys J Plus, 2019, 134(7): 333.
[4] SIRUNYAN A M, TUMASYAN A, ADAM W et al. JINST, 2020, 15(09): P09018.
[5] MAJUMDAR K. J Phys Conf Ser, 2015, 598(1): 012023.
[6] ARMATOL A, ARMENGAUD E, ARMSTRONG W, et al. arXiv: 2011.11726, 2020.
[7] SIRUNYAN A, TUMASYAN A, ADAM W, et al.Journal of Instrumentation, 2017, 12(10): P10003.
[8] KOCH L, DENIG A, DREXLER P, et al. Journal of Instrumentation, 2017, 12(07): C07001.
[9] NAKHOSTIN M. Nuclear Engineering and Technology, 2020, 52 (2): 360.
[10] LEE M, LEE D, KO E, et al. Nuclear Engineering and Technology, 2020, 52(5): 1029.

[11] CASIMIRO E, ANJOS J C. Journal of Physics: Conference Series, 2008, 116: 012003.
[12] CAO J, LUK K B. Nuclear Physics B, 2016, 908: 62.
[13] AN F, BALANTEKIN A, BAND H, et al. Nucl Instr and Meth A, 2015, 773: 8.
[14] SUZUKI A. The European Physical Journal C, 2014, 74(10).
[15] COLLABORATION R, AHN J K. arXiv: 1003.1391, 2010.
[16] LUNDY R A. Phys Rev, 1962, 12: 1686.
[17] BARDIN G, DUCLOS J, MAGNON A, et al. Phys Lett B, 1984, 137 (1): 135.
[18] CHITWOOD D B, BANKS T I, BARNES M J, et al. Phys Rev Lett, 2007, 99: 032001.
[19] ŚANCHEZ E. Physics Procedia, 2011, 17: 168.
[20] SUN Lazhen, WU Yusheng, LI Cheng. Physics Experiment Ation, 2010, 30(2): 1. (in Chinese)
(孙腊珍, 吴雨生, 李澄. 物理实验, 2010, 30(2): 1.)
[21] HALL R E, LIND D A, RISTINEN R A. American Journal of Physics, 1970, 38(10): 1196.
[22] OWENS A, MACGREGOR A E. American Journal of Physics, 1978, 46(8): 859.
[23] LEWIS R J. American Journal of Physics, 1982, 50(10): 894.
[24] COAN T, LIU T, YE J. American Journal of Physics, 2006, 74(2): 161.
[25] WEBBER D M, TISHCHENKO V, PENG Q, et al. Phys Rev Lett, 2011, 106: 041803.
[26] WANG Rong, HAN Chengdong, ZHANG Yapeng, et al. Nuclear Physics Review, 2016, 33(03): 315. (in Chinese)
(王荣, 韩成栋, 张亚鹏, 等. 原子核物理评论, 2016, 33(03): 315.)
[27] TIAN Yi, HU Luguo, SUN Baohua. College Physics, 2018, 37(10): 36. (in Chinese)
(田怡, 胡陆国, 孙保华. 大学物理, 2018, 37(10): 36.)
[28] LIN Yanchang, CHEN Shaomin, GAO Yuanning, et al. Experimental Technology and Management, 2008, 25(09): 41. (in Chinese)
(林延畅, 陈少敏, 高原宁, 等. 实验技术与管理, 2008, 25(09): 41.)
[29] WU Yusheng, LV Zhiyan, LI Shu, et al. Journal of University of Science and Technology of China, 2010, 040(006): 608. (in Chinese)
(吴雨生, 吕治严, 李数, 等. 中国科学技术大学学报, 2010, 040(006): 608.)
[30] ORGANIZATION W H. Who Handbook on Indoor Radon: a Public Health Perspective[M]. Switzerland: WHO Press, 2009: 89.
[31] PAN Z. Radiation Level in China[M]. Beijing: China Atomic Energy Publishing and Media Co., Ltd, 2011.
[32] GROUP P D, ZYLA P A, BARNETT R M, et al. Progress of Theoretical and Experimental Physics, 2020, 2020(8).
[33] AGOSTINELLI S, ALLISON J, AMAKO K, et al. Nucl Instr and Meth A, 2003, 506(3): 250.
[34] ALLISON J, AMAKO K, APOSTOLAKIS J, et al. IEEE Transactions on Nuclear Science, 2006, 53(1): 270.
[35] ALLISON J, AMAKO K, APOSTOLAKIS J, et al. Nucl Instr and Meth A, 2016, 835: 186.
[36] BARDIN G, DUCLOS J, MAGNON A, et al. Nuclear Physics A, 1981, 352(3): 365.
[37] WARD T, BARKER M, BREEDEN J, et al. American Journal of Physics, 1985, 53(6): 542.
[38] KREMER J, BOEZIO M, AMBRIOLA M L, et al. Phys Rev Lett, 1999, 83: 4241.
[39] GAISSER T K, ENGEL R, RESCONI E. Cosmicrays and Particle Physics[M]. Cambridg: Cambridge University Press, 2016.
[40] GUAN M, CHU M C, CAO J, et al. arXiv: 1509.06176, 2015.
[41] BAHMANABADI M. Nucl Instr and Meth A, 2019, 916: 1.
[42] PETHURAJ S, DATAR V, MAJUMDER G, et al. Journal of Cosmology and Astroparticle Physics, 2017, 2017(09): 021.

测量宇生μ子寿命验证堆积事例处理新方法

廖 健, 余 涛, 周逸行, 徐 宇, 陈 羽†, 唐 健†

(中山大学物理学院，广州 510275)

摘要: 提出了一种在数据分析中降低堆积事例误差的一种修正方法，并通过塑料闪烁体搭建的宇生μ子时间符合探测器开展寿命测量实验进行验证。寿命测量实验研究表明，主要本底事件来自电子学噪声和堆积事例。为了弥补在本地实验室中，μ子衰变事例在总体宇生μ子事例中较为稀有的短板，我们使用蒙特卡罗模拟程序产生大样本量，进一步验证该分析方法的有效性。修正后的最终实验结果为 $\tau_{\mu}^{\exp}=2.19\pm0.07$ μs，而修正前的实验结果为 $\tau'_{\mu}=2.27\pm0.07$ μs。(95%置信度水平)。预计，统计学处理堆积事例的方法将适用于符合测量与堆积事例伴生的同类型实验。

关键词: 宇生μ子；μ子寿命测量；符合测量本底；堆积事例

收稿日期: 2021-05-05； **修改日期:** 2021-06-20

基金项目: 国家自然科学基金资助项目 (12075326)；中山大学本科教学质量工程项目；中山大学大学生创新创业项目 (20201319)

† **通信作者:** 陈羽，E-mail：chenyu73@mail.sysu.edu.cn；唐健，E-mail：tangjian5@mail.sysu.edu.cn。